

# Kinetic Stabilization of Microtubule Dynamic Instability in Vitro by Vinblastine<sup>†</sup>

Robert J. Toso,<sup>‡</sup> Mary Ann Jordan,<sup>‡</sup> Kevin W. Farrell,<sup>‡</sup> Brian Matsumoto,<sup>§</sup> and Leslie Wilson<sup>\*‡</sup>

Division of Molecular and Cellular Biology, Department of Biological Sciences, and Neurosciences Research Institute, University of California, Santa Barbara, California 93106

Received August 27, 1992; Revised Manuscript Received November 13, 1992

**ABSTRACT:** The antiproliferative action of vinblastine at low concentrations appears to result from modulation of the polymerization dynamics of spindle microtubules rather than from depolarization of the microtubules [Jordan, M. A., Thrower, D., & Wilson, L. (1991) *Cancer Res.* 51, 2212–2222; (1992) *J. Cell. Sci.* 102, 401–416]. In the present study, we used differential interference contrast video microscopy to analyze the effects of vinblastine on the growing and shortening dynamics (dynamic instability) of individual bovine brain microtubules in vitro. With microtubules which were either depleted of microtubule-associated proteins (MAPs) or rich in MAPs, low concentrations of vinblastine (0.2  $\mu$ M–1  $\mu$ M) suppressed the growing and shortening rates and increased the percentage of time that the microtubules spent in a state of attenuated activity, neither growing nor shortening detectably. Vinblastine also suppressed the duration of microtubule growing and shortening, and increased the duration of the attenuated state, during which the microtubules neither grew nor shortened detectably. Consistent with previous data obtained using radiolabeled nucleotide exchange in microtubule suspensions [Jordan, M. A., & Wilson, L. (1990) *Biochemistry* 29, 2730–2739], vinblastine suppressed growing and shortening dynamics at the kinetically more rapid plus ends. The results suggest that vinblastine kinetically stabilizes microtubule ends by modulating the gain and loss of the stabilizing GTP or GDP-P<sub>i</sub> “cap”, which is believed to be responsible for the transitions between the growing and shortening phases. The data support the hypotheses that (1) low concentrations of vinblastine inhibit mitosis by kinetically stabilizing the polymerization dynamics of spindle microtubules and that (2) the dynamics of spindle microtubules are critical for the proper progression of mitosis.

Vinblastine, a “Vinca” alkaloid obtained from the plant *Catharanthus roseus*, is widely used for the treatment of various forms of cancer (McCormack, 1990; Rowinsky & Donehower, 1991). Like vincristine and other related Vinca alkaloids, vinblastine is a potent inhibitor of cell proliferation which arrests many mammalian cells in metaphase of mitosis by an action on microtubules [see Jordan et al. (1991, 1992)]. Vinblastine is well-known as an inhibitor of microtubule polymerization in vitro and in cells, and the results of early studies on the mechanism of mitotic inhibition by vinblastine, which involved the use of relatively high concentrations of the drug, suggested that vinblastine inhibited mitosis by depolymerizing the spindle microtubules required for chromosome movement [Bensch & Malawista, 1969; Owellen et al., 1976; reviewed in Dustin (1984)].

However, we found recently by analyzing radiolabeled guanosine 5'-triphosphate (GTP)-tubulin exchange with MAP-rich bovine brain microtubules at polymer-mass steady state in vitro that very low concentrations of vinblastine strongly inhibited both the addition and loss of tubulin at the net growing ends of the microtubules without appreciably depolymerizing the microtubules (Jordan & Wilson, 1990). In addition, we found that inhibition of mitosis in HeLa cells induced by very low vinblastine concentrations (approximately 1 nM drug in

the culture medium) occurred without detectable loss of microtubule polymer mass and with only subtle effects on the organization of the mitotic spindle microtubules and chromosomes (Jordan et al., 1991, 1992; Wendell et al., 1993). These results indicated that at low concentrations, vinblastine may act by suppressing the growing and shortening dynamics of specific mitotic microtubules and that such suppression may interfere with the mechanisms responsible for chromosome movement.

Microtubules are not simple equilibrium polymers [e.g., see Mitchison (1988), Carlier (1989), and Gelfand and Bershadsky (1991) for recent reviews]. The energy provided by hydrolysis of tubulin-liganded GTP during addition of tubulin at the microtubule ends creates phase transitions at the ends that give rise to two remarkable dynamic behaviors. One such behavior, called “dynamic instability” (Mitchison & Kirschner, 1984a,b), can be described in simple terms as a stochastic switching between shortening and growing phases at the ends of individual microtubules. A second dynamic behavior which seems to be a consequence of dynamic instability at the microtubule ends, called “treadmilling” or “flux”, is the net growing of a microtubule at one end and the net shortening at the opposite end (Margolis & Wilson, 1978). The gain and loss of a stabilizing “cap” at the microtubule ends consisting of GTP-liganded or GDP-P<sub>i</sub>-liganded tubulin is hypothesized to create dynamic instability and flux (Farrell et al., 1987).

Mitotic spindle microtubules are especially dynamic, and exchange their tubulin with tubulin in the cytoplasmic pool with half-times of less than a minute [reviewed in McIntosh and Hering (1991)]. Astral and interpolar spindle microtubules grow and shorten rapidly at their unattached plus ends, while the kinetochore microtubules also appear to grow and shorten rapidly at plus ends while the ends remain anchored

<sup>†</sup> Supported by USPHS Grant NS13560 from the National Institute of Neurological and Communicative Disorders and Stroke (L.W.), by American Cancer Society Grant CH-381 (L.W. and M.A.J.), by USPHS Grant GM41751 (K.W.F.), and by USPHS Grant EY07191 (B.M.).

<sup>‡</sup> Department of Biological Sciences.

<sup>§</sup> Neurosciences Research Institute.

<sup>1</sup> Abbreviations: DIC, differential interference contrast; EGTA, [ethyleneglycolbis(oxyethylenetriole)]tetraacetic acid; GTP, guanosine 5'-triphosphate; MAP(s), microtubule-associated protein(s); Mes, 2-(N-morpholino)ethanesulfonic acid; MEM buffer, 100 mM Mes, 1 mM EGTA, 1 mM MgSO<sub>4</sub>, and 1.0 mM GTP, pH 6.7.

at the kinetochores. In addition, kinetochore microtubules during metaphase appear to treadmill or flux, incorporating tubulin at their plus ends (at the kinetochores) and losing tubulin at their minus ends (at the spindle poles) at a rate of approximately 0.5  $\mu\text{m}/\text{min}$  (Mitchison, 1989). While it is becoming clear that molecular motors play a major role in chromosome organization and movement during mitosis by exerting force between microtubules and other mitotic components [see McIntosh and Hering (1991)], it is reasonable to think that the dynamics of the microtubules themselves may also play an important role in mitosis.

In the present work, we determined the effects of vinblastine on the dynamic instability parameters of MAP-depleted and MAP-rich microtubules in vitro by direct observation of the effects of the drug on the dynamics of individual microtubules by differential interference contrast (DIC) video microscopy. The purpose was to determine whether vinblastine could modulate microtubule dynamics in vitro in ways that might provide insight into how the drug blocks mitosis. We found that vinblastine strongly suppressed dynamic instability at the kinetically rapid plus ends of bovine brain microtubules. The data strongly support the hypotheses that kinetic stabilization of spindle microtubule dynamics is responsible for the ability of very low vinblastine concentrations to inhibit mitosis and that the polymerization dynamics of the microtubules are critical for the progression of mitosis.

## MATERIALS AND METHODS

**Preparation of MAP-Rich and MAP-Depleted Microtubule Protein.** MAP<sup>1</sup>-rich bovine brain microtubule protein (70% tubulin, 30% MAPs) was isolated without glycerol by 3 cycles of polymerization and depolymerization in vitro by a modification (Farrell & Wilson, 1984) of the procedure of Asnes and Wilson (1979). The protein was stored frozen as microtubule pellets at  $-70^{\circ}\text{C}$ .

MAP-depleted tubulin was prepared from the MAP-rich microtubule protein based on the method of Mitchison and Kirschner (1984a). MAP-rich microtubule protein pellets were thawed and resuspended by Dounce homogenization in 100 mM Mes, 1 mM EGTA, and 1 mM  $\text{MgSO}_4$ , pH 6.7, containing 1.0 mM GTP (MEM buffer). Solutions were clarified by centrifugation at 150000g for 30 min,  $4^{\circ}\text{C}$  (Beckman 50Ti rotor), and applied to a 30-mL Whatman P-11 column (50–60 mg total protein) equilibrated with the same buffer. Peak flow-through fractions were pooled, the  $\text{MgSO}_4$  concentration was readjusted to 1 mM, and the solution was quick-frozen as drops in liquid nitrogen and stored at  $-70^{\circ}\text{C}$  until used. Tubulin prepared in this way was >99% pure. No contaminating MAPs were detectable on heavily overloaded SDS-polyacrylamide gels stained with Coomassie Blue. However, a number of MAPs were detectable, but not quantifiable, by silver staining.

**Preparation of MAP-Rich Microtubules for Video Microscopy.** Pellets of MAP-rich microtubule protein were resuspended by Dounce homogenization in MEM buffer containing 1 mM GTP and incubated for 10 min at  $4^{\circ}\text{C}$ . The protein solution was adjusted to 1 mg/mL total protein, and polymerization was initiated by warming to  $30^{\circ}\text{C}$ . Video microscopy was carried out between 30 and 90 min after initiation of polymerization to ensure that the microtubules were at polymer-mass steady state for the duration of the experiment. In experiments with MAP-rich microtubules, the length change data represent the total combined length changes at both ends of the individual microtubules. It was not possible to analyze the growing and shortening dynamics

at the individual ends of MAP-rich microtubules using flagellar axonemal seeds to mark the ends (see below) because extensive self-nucleation obscured the microtubules seeded by the axonemes.

**MAP-Depleted Microtubules.** Pellets of MAP-depleted tubulin were thawed, incubated for 10 min at  $0^{\circ}\text{C}$ , and diluted 8–10-fold (v/v) to a concentration of 1.5 mg/mL in MEM buffer containing 1 mM GTP. For analysis of dynamic instability at microtubule plus ends, the MAP-depleted microtubules were grown onto the ends of flagellar axonemal seeds that had been purified from sea urchin (*Strongylocentrotus purpuratus*) sperm by the method of Farrell and Wilson (1978).

In early experiments, we polymerized microtubules onto flagellar seeds at relatively high tubulin concentration and diluted them into a tubulin solution at the critical subunit concentration. However, for reasons we do not understand, the microtubules when visualized by video microscopy did not remain at polymer-mass steady state. Instead, they underwent continuous net depolymerization at a mean rate of >11 000 tubulin dimers per minute per microtubule. Under such net depolymerization conditions, the action of low vinblastine concentrations was difficult to detect and quantitate. We found that the most sensitive condition for visualizing the action of vinblastine on microtubule growing and shortening dynamics was with a system that had nearly attained polymer-mass steady state. Such a condition was attained by polymerizing MAP-depleted tubulin onto the axonemal seeds at a protein concentration of 1.5 mg/mL. In this concentration range, the tubulin did not self-nucleate, and polymerization occurred only at the ends of axonemal seeds. The seed concentration was adjusted by trial and error to yield a density of approximately 2–5 axonemes per microscope field which was optimal for visualizing the microtubules. Growing and shortening dynamics were analyzed at the minus ends of microtubules seeded with short fragments of stable outer-doublet microtubules prepared by the method of Wilson and Meza (1973).

The growing and shortening dynamics of entire MAP-depleted microtubules were also analyzed. Such microtubules were nucleated using sheared MAP-depleted microtubule seeds (final concentration 2–5 mg/mL; mean length <1  $\mu\text{m}$ ) prepared by polymerizing MAP-depleted tubulin in the presence of 1 M sodium glutamate or 3 M glycerol as described by Walker et al. (1988).

For experiments in which the effects of vinblastine on the growing and shortening dynamics were examined, the protein solutions prepared as described above were polymerized in the continuous presence of vinblastine (a generous gift from the Lilly Research Laboratories, Indianapolis, IN) at the desired concentration.

Protein was determined by the method of Bradford (1976) using bovine serum albumin as the standard.

**Video Microscopy.** The growing and shortening dynamics of individual microtubules were visualized by video-enhanced DIC microscopy. A 2- $\mu\text{L}$  volume of microtubule suspension was pipetted on a 12-mm-diameter circular glass coverslip that was prewarmed to  $30^{\circ}\text{C}$ . The microtubule suspension was then sandwiched between the coverslip and a second, 18-mm circular prewarmed glass coverslip, and the entire "sandwich" was sealed on a prewarmed glass slide with high-viscosity immersion oil which had been clarified by centrifugation at 20000g for 30 min (Sorvall RC 5B centrifuge, SS-34 rotor) to remove particulate material. Limiting the volume applied to the coverslips to 2  $\mu\text{L}$  minimized microtubule

drift while the immersion oil seal prevented the microtubule suspension from drying out.

DIC video microscopy was carried out at 30 °C using a Zeiss IM 35 microscope equipped with a Zeiss Planapo 63× 1.4-na oil immersion objective and a temperature-controlled microscope stage and a 100-W mercury lamp. Images were captured in real time using a Hamamatsu C2400 (Newvicon) video camera equipped with a camera controller that included adjustable gain and offset controls. The camera output was observed on a Sony Model PVM122 high-resolution monitor, and data were recorded with a JVC HRs5800u super VHS video cassette recorder. All electrical equipment was isolated with line voltage regulators.

Measurements of microtubule lengths were made at 15-s intervals using an IBM AT personal computer equipped with a Targa-M8 frame-grabber (Tru-vision) and JAVA video analysis software (Jandel Scientific). Microtubule images from the video output were "frozen" on the computer screen, and microtubule lengths were measured and recorded in a database by tracing the microtubule from one end to the other using a "mouse". All measurements were made at least twice and usually 3 or more times at each time point, and the microtubules often were remeasured on a different day to ensure maximal accuracy. Microtubules were measured until they depolymerized completely or until the image became obscured so that the error of measurement increased to  $>0.2 \mu\text{m}$ . An average of 7 microtubules from a minimum of 2 experiments comprising at least 100 total measurements was used to calculate the results for each experimental condition. Growing and shortening rates were calculated using a conversion factor of  $1 \mu\text{m}$  of microtubule length = 1690 tubulin dimers (Amos & Klug, 1974). Length calibration of video images was accomplished by video recording a length standard at the same magnification used for experimental observations.

## RESULTS

### Dynamic Instability Parameters of MAP-Depleted Microtubules: Suppression of Dynamics by Vinblastine

**Dynamic Instability Parameters of MAP-Depleted Microtubules.** When MAP-depleted bovine brain tubulin was polymerized at the ends of axonemal seeds (Materials and Methods), microtubule growth occurred predominantly at the plus ends as determined by the relative lengths of the microtubules at the opposite ends of the individual axonemes (Walker et al., 1988; Gildersleeve et al., 1992). Microtubules also formed at the minus ends, but usually only one microtubule formed per minus end, and its length rarely exceeded  $1 \mu\text{m}$ . Under the conditions used, the plus-end microtubules underwent slow net growth at a constant mean rate of approximately  $11 \pm 1$  tubulin dimers  $\text{s}^{-1}$  microtubule $^{-1}$  for the period between 0 and 60 min after observation was initiated. This represents mean net growth of  $0.1 \mu\text{m}$  in 15 s, which is below the resolution of the microscope and is scored as no change by our measurement protocol.

As described by others (Walker et al., 1988; Gildersleeve et al., 1992), the microtubules seeded at the plus ends of the axonemes displayed growing and shortening dynamics that could be monitored and analyzed quantitatively by DIC video microscopy. Typical examples of the growing and shortening dynamics displayed by individual MAP-depleted control microtubules (no vinblastine) are shown in Figure 1A. The mean values for all of the dynamic instability parameters analyzed in the present work for the plus ends of control microtubules are summarized in Table I. As documented

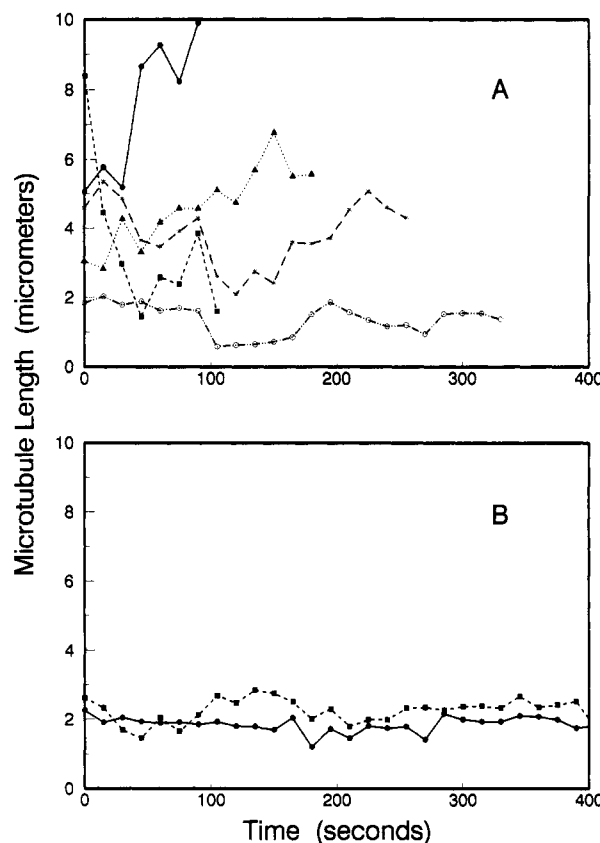


FIGURE 1: Changes in microtubule lengths in the absence (A) and presence (B) of  $0.5 \mu\text{M}$  vinblastine. MAP-depleted microtubules were polymerized at the plus ends of axonemal seeds in the absence or presence of  $0.5 \mu\text{M}$  vinblastine. The growing and shortening dynamics were analyzed as described under Materials and Methods. Each tracing shows the growing and shortening dynamics of an individual microtubule.

Table I: Dynamic Instability Parameters at Plus Ends of Individual MAP-Depleted Brain Microtubules<sup>a</sup>

parameter	value
mean rates ( $\text{s}^{-1}$ )	
growing	$106 \pm 13$
shortening	$104 \pm 16$
mean phase durations (s)	
growing	$27 \pm 3$
shortening	$20 \pm 2$
attenuation <sup>b</sup>	$21 \pm 5$
total time (%)	
growing	$48 \pm 5$
shortening	$35 \pm 5$
attenuation	$19 \pm 3$
dynamicity <sup>c</sup> ( $\text{s}^{-1}$ )	$83 \pm 8$

<sup>a</sup> Dynamic instability parameters of MAP-depleted bovine brain microtubules grown at the plus ends of flagellar axonemal seeds were determined as described under Materials and Methods. Values are the mean  $\pm$  standard error of the mean. <sup>b</sup> Mean time that the microtubule spent neither growing nor shortening detectably. <sup>c</sup> Total tubulin dimer exchange calculated from total detectable growing and shortening.

previously by Gildersleeve et al. (1992), individual microtubules displayed wide variation in their growing and shortening rates (Figures 1A and 2A). For example, growing rates ranged from a high value of  $390$  dimers  $\text{s}^{-1}$  microtubule $^{-1}$  to a low value of  $23$  tubulin dimers  $\text{s}^{-1}$ , the lowest rate detectable with 15-s sampling times (Figure 2A).

Control microtubules also displayed wide variation in the percentage of time spent in an attenuated state (Figure 1A). Under the conditions used in the present study, on average the plus-end microtubules spent approximately 19% of the total

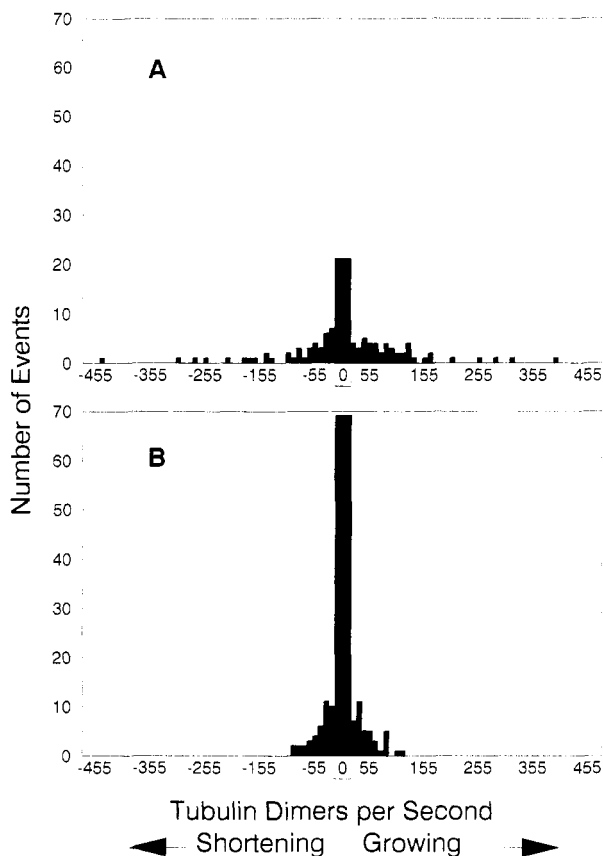


FIGURE 2: Distribution of growing and shortening rates at the plus ends of MAP-depleted microtubules in the absence (A) and presence (B) of  $0.5 \mu\text{M}$  vinblastine. Positive rates = growing; negative rates = shortening; rates between  $+23$  and  $-23$  dimers  $\text{s}^{-1}$  were below the resolution of the microscope and are reported as zero.

time neither growing nor shortening detectably (Table I). Walker et al. (1988) have called this a "pause" state and reported that under the conditions used in their studies, microtubules spent  $<1\%$  of the total time in a pause state. In the present work, we call this a state of attenuated activity or an attenuation state, rather than a pause state, because growing and shortening may be occurring that are below the level of detection by the video system ( $0.2 \mu\text{m}$ ). Thus, the time the microtubules are reported as spending in the attenuated state should be considered in the present study as representing an unknown combination of very slow growing, very slow shortening, and, perhaps, no growing or shortening.

**Suppression of Dynamic Instability at Plus Ends of MAP-Depleted Microtubules by Vinblastine.** The suppression of growing and shortening dynamics of individual microtubules by vinblastine can be visualized readily by comparing the length changes with time of control microtubules (Figure 1A) with the length changes with time in the presence of  $0.5 \mu\text{M}$  vinblastine (Figure 1B). For example, it is clear that the percentage of time individual microtubules spent in a state of attenuated activity in the presence of the drug, neither growing nor shortening detectably, was greatly increased as compared with control microtubules (see below).

A histogram of the rates of growing and shortening in the presence of  $0.5 \mu\text{M}$  vinblastine is shown in Figure 2B. It is clear by comparing these data with the rates for control microtubules (Figure 2A) that vinblastine strongly decreased both the shortening and the growing rates. For example, the maximal shortening and growing rates were decreased by the drug from approximately  $445$  and  $390$  tubulin dimers  $\text{s}^{-1}$ , respectively, to approximately  $95$  and  $120$  dimers  $\text{s}^{-1}$ , respec-

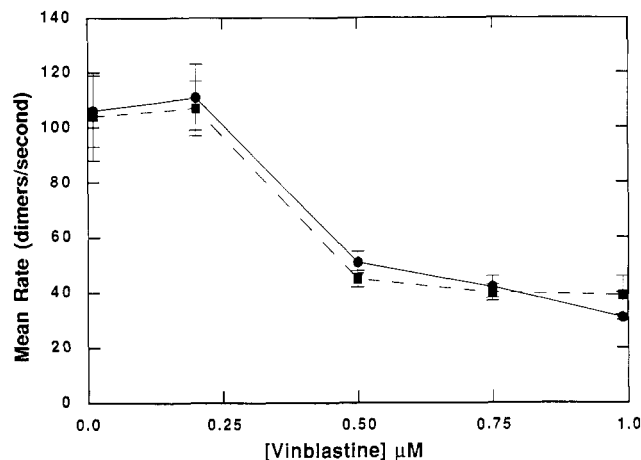


FIGURE 3: Effects of vinblastine concentration on the mean growing and shortening rates at the plus ends of MAP-depleted microtubules. Mean growing rates (squares) and shortening rates (circles) of individual microtubules were determined in the absence or presence of different vinblastine concentrations (Materials and Methods). Error bars = standard error of the mean.

tively. Suppression of the mean growing and shortening rates is shown as a function of vinblastine concentration in Figure 3. Both the mean growing and mean shortening rates were reduced by the drug in a concentration-dependent manner. In addition, individual vinblastine concentrations suppressed both rates to similar extents.

The concentration range required for vinblastine to exert its suppressive effects was narrow. For example, no suppression of growing rates was detectable at  $0.2 \mu\text{M}$  vinblastine, while approximately 50% inhibition of both rates occurred at  $0.5 \mu\text{M}$  drug. At  $1 \mu\text{M}$  vinblastine, the mean shortening rate was reduced by 63% from  $104$  to  $39$  tubulin dimers  $\text{s}^{-1}$ , and the mean growing rate was reduced by 71% from  $106$  to  $31$  tubulin dimers  $\text{s}^{-1}$ . It was not possible to analyze the effects of vinblastine on the dynamic instability parameters at concentrations higher than  $1 \mu\text{M}$ . Such concentrations of vinblastine induced splaying and peeling of protofilaments at the microtubule ends due to the interaction of vinblastine with low-affinity sites located along the microtubule surface (Jordan et al., 1986; Singer et al., 1989). The ends of microtubules with splayed protofilaments appeared diffuse when visualized by video microscopy, making precise length measurements impossible.

Vinblastine also affected the durations of the growing, shortening, and attenuation phases. These effects of vinblastine are potentially very important because they indicate that the drug may be affecting the mechanism responsible for gain and loss of the stabilizing "cap" at the plus ends. Vinblastine decreased the mean durations of the shortening and growing phases (Figure 4). For example, at  $1 \mu\text{M}$  vinblastine, the mean duration of the shortening phase appears to have been reduced slightly from  $20$  to  $16$  s, and the mean duration of the growing phase was reduced by 33% from  $27$  to  $15$  s. Vinblastine strongly increased the mean duration of the attenuation phase (Figure 4). For example,  $1 \mu\text{M}$  vinblastine increased the attenuation phase duration by a factor of 3 from  $21$  to  $64$  s.

The effects of vinblastine on the frequency of switching among phases, calculated from the mean phase duration data, are shown in Table II. Vinblastine increased the switching frequency from shortening to growing or attenuation. This parameter is the equivalent of "rescue" using the terminology.

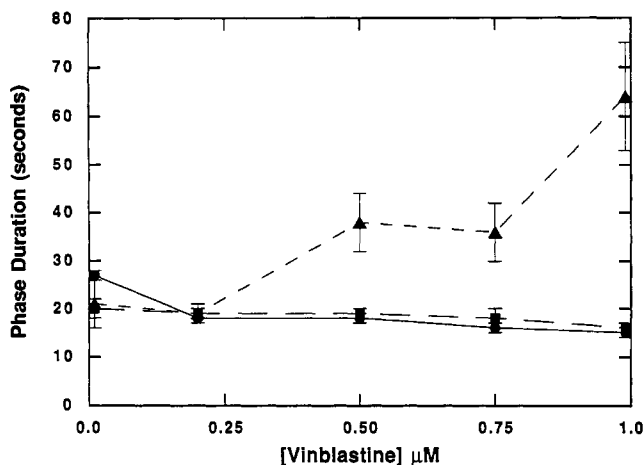


FIGURE 4: Effects of vinblastine concentration on the mean phase durations at the plus ends of MAP-depleted microtubules. The mean lengths of time individual microtubules spent in the growing (circles), shortening (squares), or attenuation phases (triangles) were determined in the absence and presence of different vinblastine concentrations (Materials and Methods). Error bars = standard error of the mean.

Table II: Effects of Vinblastine on the Transition Frequencies at Microtubule Ends<sup>a</sup>

vinblastine concn (μM)	transition frequencies (mean no. of events/min)			
	from S to G or A	from G or A to S	from A to G or S	from G or S to A
MAP-Depleted Microtubules				
0 (control)	3.0	1.6	2.9	0.65
0.2	3.2	2.0	3.2	0.89
0.5	3.2	1.2	1.6	1.4
0.75	3.4	0.94	1.7	2.7
1.0	3.8	0.56	1.0	2.7
MAP-Rich Microtubules				
0 (control)	3.3	1.1	2.5	2.2
1	3.3	0.25	0.54	3.8

<sup>a</sup> G = growing phase, S = shortening phase, A = attenuation phase. Transition frequencies were calculated by dividing the number of times the transition occurred by the total time that the microtubule spent in the phase or phases from which the transition occurred. For example, the transition from S to either A or G is equal to the number of shortening events divided by the total time spent shortening. This parameter is equivalent to the inverse of the mean phase duration for shortening. The transition to S (either from A or from G) equals the number of shortening events divided by the total time spent in attenuation or growing; i.e., frequency of transition into shortening = (fraction of total time spent shortening/average duration of shortening)/fraction of total time spent growing or in attenuation.

of Walker et al. (1988), which may represent the frequency for regain of the stabilizing "cap" at microtubule plus ends. In addition, while 0.2 μM vinblastine may have increased the switching frequency from growing or attenuation to shortening somewhat, at the higher concentrations examined, vinblastine clearly decreased the switching frequency from growing or attenuation to shortening (Table II). This parameter is the equivalent of "catastrophe" using the terminology of Walker et al. (1988), and it may represent the frequency of cap loss at plus ends. Thus, at concentrations of 0.5 μM and higher, vinblastine may increase the rate of regain and decrease the rate of loss of the stabilizing cap at the plus ends.

It is also clear that vinblastine strongly decreased the frequency of switching from the attenuated state to growing or shortening and, reciprocally, strongly increased the frequency of switching from growing or shortening to the attenuated state (Table II). These data demonstrate that the drug kinetically stabilizes microtubule plus ends, reducing

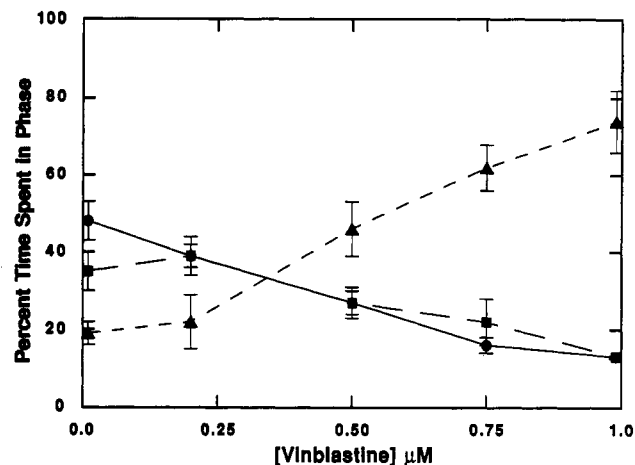


FIGURE 5: Effects of vinblastine concentration on the percent of total time MAP-depleted plus-end microtubules spent growing, shortening, or in an attenuated state. The mean percentage of time microtubule plus ends spent growing (circles), shortening (squares), or in an attenuated state (triangles) is shown in relation to the total amount of time in all phases in the absence and presence of different concentrations of vinblastine. Error bars = standard error of the mean.

the gain and loss of tubulin dimers to below levels detectable by video microscopy.

Vinblastine strongly increased the percentage of total time the microtubules spent in an attenuated state and correspondingly decreased the percentage of total time the microtubules spent growing and shortening (Figure 5). For example, in the presence of 1 μM vinblastine, microtubules spent 74% of the total time in a state in which no length changes were detectable by video microscopy as compared with 19% for control microtubules.

The overall mean rate of tubulin exchange at microtubule ends, calculated from all detectable growing and shortening events and including the time the microtubules are in the attenuated state (calculated as a rate of zero), can provide a quantitative measure of the overall dynamic activity of the end. This parameter, which we have called the "dynamicity" (see also Table I), provides a useful quantitative measure of the overall inhibitory activity which substances such as vinblastine exert on visible tubulin exchange at microtubule ends. As can be seen in Figure 6, vinblastine reduced the dynamicity of the plus ends in a concentration-dependent manner, with 1 μM vinblastine reducing this parameter by approximately 89% from 83 to 9 tubulin dimers s<sup>-1</sup> end<sup>-1</sup>.

Under the conditions used in the present study, the control microtubules displayed slow net growth, and as expected, vinblastine reduced this growth rate (Table III). The slow net growth of control microtubules was reduced by 80% at the lowest vinblastine concentration examined (0.2 μM) from approximately 11 to 2 dimers s<sup>-1</sup>. The plus ends then appeared to remain within 2 dimers s<sup>-1</sup> of no net growth or shortening as the vinblastine concentration was increased to 1 μM, the highest vinblastine concentration tested.

**Effects of Vinblastine on Growing and Shortening Dynamics at Minus Ends of MAP-Depleted Microtubules.** We also attempted to measure the effects of vinblastine on growing and shortening dynamics at the minus ends of microtubules. As indicated, only very short microtubules (<1 μm in length) formed at the minus ends of axonemes under the conditions used, which could not be measured accurately using axoneme seeds because of their short lengths. By using purified outer doublet microtubules (Wilson & Meza, 1973) instead of axonemes to nucleate MAP-depleted microtubules, we found

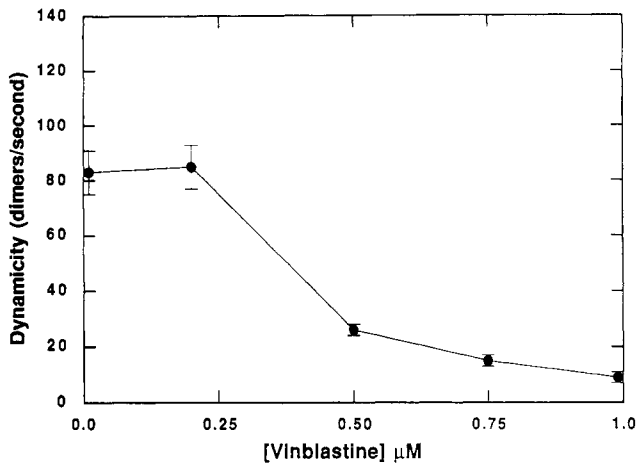


FIGURE 6: Effects of vinblastine concentration on the overall dynamicity of MAP-depleted microtubules at their plus ends. The mean rate of tubulin exchange at microtubule ends, calculated from all detectable growing and shortening events, including the time in the attenuated state which was calculated as zero, is shown in the absence and presence of different concentrations of vinblastine. Error bars = standard error of the mean.

Table III: Net Mean Growing or Shortening of Microtubules in the Absence and Presence of Vinblastine<sup>a</sup>

vinblastine concn ( $\mu\text{M}$ )	net growing or shortening (dimers $\text{s}^{-1}$ )
control (no vinblastine)	+11 $\pm$ 1
0.2	+2 $\pm$ 2
0.5	+1 $\pm$ 1
0.75	-2 $\pm$ 2
1.0	-1 $\pm$ 1

<sup>a</sup> The total net growth or shortening of the microtubule plus ends observed in the absence and presence of different vinblastine concentrations was calculated from the growing and shortening rate. The attenuation phase was calculated as a rate of zero.

we could define the ends of the minus-end microtubules more precisely and measure their growing and shortening dynamics.

The dynamics of such minus-end microtubules in the absence of vinblastine were very strongly attenuated as compared with the dynamics of microtubules grown at the plus ends of outer doublet microtubules or axonemes. For example, the mean growing rate at the minus end was  $34 \pm 4$  dimers  $\text{s}^{-1}$ , and the mean shortening rate was  $29 \pm 1$  dimers  $\text{s}^{-1}$ . Most significantly, the minus-end microtubules spent 94% of the time in an attenuated phase, neither growing nor shortening. The slow dynamics at minus ends under the conditions used made it impossible to analyze the effects of vinblastine at these ends.

**Suppression of Dynamic Instability by Vinblastine of Homogeneous (Not Axoneme-Seeded) MAP-Depleted Microtubules.** We also analyzed the dynamics of homogeneous MAP-depleted microtubules. With such microtubules, the dynamics represent the combined events at both microtubule ends; the dynamics at the individual ends cannot be distinguished. The dynamic instability parameters of the homogeneous non-axoneme-seeded microtubules were indistinguishable from those at the plus ends of the seeded microtubules both in the absence and in the presence of several concentrations of vinblastine (data not shown). Therefore, the minus ends of the homogeneous microtubules must be significantly less active kinetically than the plus ends, and the growing and shortening dynamics of these microtubules must primarily represent the dynamics at the plus ends. In further support of the foregoing interpretation, the dynamics of the minus

Table IV: Dynamic Instability Parameters of MAP-Rich Brain Microtubules in the Presence and Absence of 1.0  $\mu\text{M}$  Vinblastine<sup>a</sup>

	controls	vinblastine
mean growing rate	47 $\pm$ 4 <sup>b</sup>	40 $\pm$ 7 <sup>b</sup>
mean shortening rate	44 $\pm$ 4 <sup>b</sup>	31 $\pm$ 2 <sup>b</sup>
mean growing time	18 $\pm$ 2 <sup>c</sup>	15 $\pm$ 1 <sup>c</sup>
mean shortening time	18 $\pm$ 1 <sup>c</sup>	18 $\pm$ 2 <sup>c</sup>
mean attenuation time	24 $\pm$ 2 <sup>c</sup>	107 $\pm$ 48 <sup>c</sup>
% of time growing	29 $\pm$ 2 <sup>d</sup>	6 $\pm$ 5 <sup>d</sup>
% of time shortening	24 $\pm$ 4 <sup>d</sup>	7 $\pm$ 2 <sup>d</sup>
% of time in attenuated state <sup>e</sup>	47 $\pm$ 6 <sup>d</sup>	88 $\pm$ 5 <sup>d</sup>
dynamicity <sup>f</sup>	24 $\pm$ 3 <sup>b</sup>	4 $\pm$ 1 <sup>b</sup>

<sup>a</sup> Dynamic instability parameters of MAP-rich bovine brain microtubules were determined as described under Materials and Methods. Values are the mean  $\pm$  standard error of the mean. <sup>b</sup> Tubulin dimers per second. <sup>c</sup> Seconds. <sup>d</sup> Percent. <sup>e</sup> Percentage of time the microtubule spends neither growing nor shortening detectably. <sup>f</sup> The mean rate of total tubulin exchange, calculated from all detectable growing, shortening, and attenuation events (during the attenuated state, the rate was calculated as zero).

ends of axoneme-seeded MAP-depleted microtubules under the conditions studied were significantly less active than the plus ends.

#### *Dynamic Instability Parameters of MAP-Rich Microtubules: Suppression of Dynamics by Vinblastine*

While the dynamic instability behavior of MAP-rich brain microtubules is extremely suppressed by the MAPs [e.g., see Horio and Hotani (1986), Hotani and Horio (1988), Farrell et al. (1987), and Jordan and Wilson (1990)], in the present study we found that we could detect and quantitate a small extent of dynamic instability behavior with MAP-rich microtubules, which provided an opportunity to analyze the effects of vinblastine on the dynamics of MAP-rich microtubules (Table IV). As compared with the dynamics of MAP-depleted control microtubules (Table I), the presence of the MAPs strongly suppressed the mean growing and shortening rates, they decreased the fraction of time the microtubules spent growing and shortening, and they increased the fraction of time the microtubules spent in the attenuated state. The strong suppression of growing and shortening rates coupled with the large increase in the percentage of time the microtubules spent in the attenuated state appears to be responsible for the shortness and relative infrequency of growing and shortening excursions which occur at the plus ends of MAP-rich microtubules.

Addition of 1  $\mu\text{M}$  vinblastine to MAP-rich microtubules further suppressed the mean growing and shortening rates and the fraction of time the microtubules spent growing and shortening (Table IV). In addition, vinblastine strongly increased the mean attenuation phase duration and the percentage of time the microtubules spent in the attenuated state. The potent ability of vinblastine to further suppress the dynamics of the already kinetically stabilized MAP-rich microtubules is shown clearly by the 88% decrease in dynamicity of the microtubules (Tables I and IV).

## DISCUSSION

In the present study, we analyzed the effects of vinblastine on dynamic instability behavior at the ends of MAP-depleted and MAP-rich bovine brain microtubules in vitro by DIC video microscopy. We found that with both microtubule preparations, concentrations of vinblastine between 0.2 and 1  $\mu\text{M}$  suppressed dynamic instability. Vinblastine strongly suppressed the growing and shortening rates, increased the

mean duration of time that the microtubules spent in an attenuated state, neither growing nor shortening detectably, and increased the percentage of total time that the microtubules spent in the attenuated state.

**Dynamics of MAP-Depleted Microtubules: Suppression by Vinblastine.** For these studies, we used MAP-depleted bovine brain microtubules that were seeded at the plus ends of flagellar axonemes under conditions that maintained slow constant net growth of the microtubules. The microtubules displayed growing and shortening dynamics of variable rate and duration that were similar to those observed previously (Horio & Hotani, 1986; Walker et al., 1988; Gildersleeve et al., 1992). However, the magnitudes of the dynamic instability parameters in the present study also differed in several ways from those reported earlier. For example, the mean duration of the growing phase in the present work (27 s at the plus ends) was shorter than that reported by others [for example, 2.9 min, in Horio and Hotani (1986); similar growing durations appear in Figure 3A of Gildersleeve et al. (1992)]. In addition, in contrast with the results of other studies [e.g., see Walker et al. (1988)], on average the microtubules in the present study spent an appreciable percentage of time in a state of attenuated activity.

There are several possible explanations for the differences. In the present work, we measured shortening, growing, and attenuation events at 15-s intervals. This procedure enabled us to compare phase durations directly. However, depolymerization or polymerization events that lasted for relatively short periods of time (<15 s) would have been underestimated. In addition, differences may exist in the dynamic behavior of the microtubules used in the present work from those used in other studies because of the use of different buffer systems or different temperatures or the presence of contaminating MAPs. In addition, in order to ensure that the microtubules were close to steady state, we initiated polymerization at low tubulin concentration (15  $\mu$ M) and monitored microtubule dynamics only after their initial assembly was complete (30–90 min after initiation); it is conceivable that under these conditions the microtubule ends may exhibit more moderate dynamic behavior than during net assembly or disassembly (Farrell et al., 1987).

Vinblastine strongly suppressed both the growing and shortening rates of the MAP-depleted microtubules at their plus ends in a concentration-dependent manner (Figure 3). Interestingly, growing and shortening rates were inhibited approximately to the same degree at each vinblastine concentration tested. Such a relatively similar degree of inhibition of shortening and growing rates by vinblastine may in large part explain why low concentrations of the drug inhibit the rate of microtubule formation, but once the microtubules are formed, the drug does not induce appreciable microtubule depolymerization (Wilson et al., 1976; Jordan & Wilson, 1990). It is worth noting that the widely-held notion that vinblastine blocks mitosis by depolymerizing microtubules derives from experiments *in vitro* and *in vivo* employing high concentrations of vinblastine [e.g., see Bensch and Malawista (1969) and Owellen et al. (1976)]. Vinblastine concentrations greater than 1  $\mu$ M cause extensive microtubule depolymerization by inducing peeling of protofilaments at both microtubule ends. This effect appears to be distinct from the kinetic stabilization of microtubules induced by low vinblastine concentrations (<1  $\mu$ M vinblastine) and is most likely a consequence of vinblastine binding to low-affinity tubulin binding sites along the microtubule surface (Jordan et al., 1986; Singer et al., 1989).

One of the most striking effects of vinblastine was to increase the percent of time microtubules spent in a state of attenuated activity and to decrease the percent of time the microtubules spent growing and shortening. The percent time spent in the attenuated state increased with increasing vinblastine concentration, rising from 22% at 0.2  $\mu$ M to 74% at 1  $\mu$ M vinblastine. Vinblastine also increased the duration of an average attenuation phase from 19 s at 0.2  $\mu$ M vinblastine to 64 s at 1  $\mu$ M vinblastine. Concomitantly, the mean duration of the growing phase was reduced from 27 to 15 s, and the mean duration of the shortening phase was reduced from 20 to 16 s.

It is conceivable that the increase in the mean duration of the attenuation phase is a consequence of the suppression of growing and shortening rates by vinblastine. As the rates decrease to below approximately 23 tubulin dimers  $s^{-1}$  (a change of <0.2  $\mu$ m in 15 s), length changes become undetectable by video microscopy. However, slow changes in net growing or shortening will become visible if they occur for long enough periods of time. For example, we detected such continuous slow depolymerization at the minus ends of MAP-depleted microtubules (data not shown), and microtubules incubated with 1  $\mu$ M vinblastine usually remained at the same length in the attenuation phase for long periods of time, as long as 3 min in some cases (data not shown). Thus, the vinblastine-induced increase in the mean duration of the attenuation phase may be due to a complete block of growing and shortening (see below).

We were unable to detect an effect of vinblastine at the kinetically slow minus ends. However, because the minus-end microtubules were very short and because their dynamics were so slow, we cannot, therefore, exclude the possibility that vinblastine might also suppress dynamics at minus ends.

**Dynamic Instability of MAP-Rich Microtubules: Suppression by Vinblastine.** In previous studies in which the length distributions of MAP-rich microtubules were measured by electron microscopy at various times after the microtubules attained polymer-mass steady state, the mean lengths and the length distributions remained constant (Wilson & Farrell, 1986; Farrell et al., 1987; Jordan & Wilson, 1990), suggesting that little or no dynamic instability behavior was occurring. The method of determining microtubule length distributions by electron microscopy is a relatively insensitive assay of dynamic instability, however, because extensive shortening and growth of a large proportion of microtubules in the population would be required to produce a detectable change in the overall length distribution. Small extents of dynamic instability would not, therefore, be detectable by this method. The far more sensitive method of measuring the incorporation and loss of radiolabeled GTP-tubulin into steady-state microtubules, in contrast, suggested that a small extent of dynamic instability was, in fact, occurring in MAP-rich microtubule populations (Wilson & Farrell, 1986; Farrell et al., 1987; Jordan & Wilson, 1990). In the present study, we were able to visualize and quantitate a limited extent of dynamic instability at the ends of MAP-rich microtubules.

The principle effects of the MAPs were to decrease the growing and shortening rates and to increase the percentage of time the microtubules spent in an attenuated state (Tables I and IV). It is interesting that although MAP-rich microtubules spent a higher percentage of time in the attenuated state than MAP-depleted microtubules, the mean durations of the attenuation phases were similar for the two microtubule systems. When vinblastine was added to MAP-rich microtubules, the most dramatic effect was the increase in mean



attenuation phase duration (Table IV). Most of the characterized brain MAPs appear to bind to the sides of microtubules, while at the concentrations used in the present study, vinblastine binds specifically to the microtubule ends (Wilson et al., 1982). Thus, the ability to increase the mean duration of the attenuation phase may be a common property of drugs such as vinblastine and colchicine associated with binding of the drug to the end of the microtubule (R. Toso, M. A. Jordan, and L. Wilson, unpublished results).

**Mechanism of Kinetic Suppression of Tubulin Exchange at Microtubule Plus Ends by Vinblastine.** Inhibition of tubulin exchange at microtubule ends at low vinblastine concentrations appears to be caused by the rapid and reversible binding of a small number of vinblastine molecules to relatively high-affinity tubulin binding sites located at 1 or both microtubule ends (approximately 17 binding sites per microtubule,  $K_D = 1.9 \mu\text{M}$ ; Wilson et al., 1982). The binding of approximately one to two molecules of vinblastine per microtubule is sufficient to inhibit the net incorporation of tubulin at microtubule plus ends at polymer-mass steady state by 50% (Wilson et al., 1982). Na and Timasheff (1980a,b) made the important discovery that vinblastine induces an isodesmic self-association of tubulin which is accompanied by a large increase in the affinity of tubulin for itself [reviewed in Timasheff et al. (1991)]. In addition, the vinblastine-induced self-association of tubulin results in a large increase in the affinity of tubulin for vinblastine. Thus, the affinity of vinblastine for self-associated tubulin may be much stronger than the affinity of vinblastine for free tubulin dimers. This phenomenon appears to explain why low concentrations of vinblastine bind preferentially to polymerized, as opposed to soluble, tubulin (Wilson et al., 1982).

How does vinblastine inhibit both the association and the dissociation of tubulin at microtubule plus ends? A reasonable explanation for how vinblastine inhibits tubulin association is that either the drug might sterically prevent further tubulin addition when it is bound at the end in the vicinity of a tubulin association site or it might induce a conformational change in the tubulin association site that prevents tubulin addition. To explain why vinblastine slows the rate of tubulin dissociation, a reasonable possibility consistent with the results of Na and Timasheff (1980a,b) and Timasheff et al. (1991) is that the drug induces a conformational change in the tubulin at the microtubule end which increases the affinity of the tubulin for adjacent tubulin molecules in the microtubule wall.

When colchicine-tubulin complex adds to microtubule ends, it does not completely inactivate the ends, but eventually it becomes buried in the microtubule as new free tubulin adds onto the end (Sternlicht & Ringel, 1979; Farrell & Wilson, 1984; Skoufias & Wilson, 1992). However, vinblastine does not become buried in the core of the microtubule but, rather, remains strictly at the microtubule ends (Jordan & Wilson, 1990). Thus, any microtubule elongation that occurs in the presence of vinblastine must require dissociation of vinblastine from the end. These results also indicate that a vinblastine-blocked tubulin addition site may be totally blocked or frozen while the vinblastine remains bound. Because 17 or so high-affinity vinblastine binding sites exist at the microtubule ends (Wilson et al., 1982), it is possible that several vinblastine molecules may be able to bind simultaneously to a single microtubule end and block more than a single tubulin addition site but that blockage of only a single tubulin addition site is sufficient to block tubulin exchange completely. Such a mechanism is consistent with that described recently in an attractive computer-simulation model of suppression of dy-

namic instability by podophyllotoxin and other antimitotic drugs (Bayley & Martin, 1991).

**Possible Effects of Vinblastine on the Gain and Loss of the Stabilizing "Cap" at Microtubule Ends.** The phase transitions between growing and shortening at microtubule ends is hypothesized to be due to the gain and loss of a stabilizing "cap" at the microtubule ends consisting of a short region of tubulin liganded with GTP or GDP- $P_i$  at the exchangeable nucleotide site (Carlier, 1989). The loss of the cap is postulated to be required for initiation of the shortening phase, and the rate-limiting step has been postulated to be a conformational change in tubulin that follows hydrolysis of GTP or the release of the  $P_i$  (Carlier, 1989; Stewart et al., 1990). Early studies demonstrated that vinblastine inhibits the GTPase activity of soluble tubulin (David-Pfeuty et al., 1979). The significance of the inhibition is not understood, but one possibility is that the drug affects GTP hydrolysis in a way that modifies the regulation of cap gain and loss.

In the present work, we found that 0.75 and 1  $\mu\text{M}$  vinblastine decreased the transition frequency at plus ends from the growing or attenuation phases into shortening (Table II), which may reflect increased retention of the stabilizing GTP or GDP- $P_i$  cap. The drug also increased the transition frequency from shortening to growing or attenuation, which may reflect gain of the stabilizing cap (Table II). Thus, one possibility is that vinblastine decreases the rate of cap loss by maintaining the tubulin-bound guanine nucleotide in the GTP or GDP- $P_i$  state. Alternatively, the conformational changes that occur in tubulin when vinblastine binds to a microtubule end may mimic the conformation of tubulin-GTP or tubulin-GDP- $P_i$  that is responsible for microtubule stabilization.

**Inhibition of Microtubule Dynamics by Vinblastine May Be the Mechanism by Which Vinblastine Induces Mitotic Block in Cells.** The data described in the present study indicate that vinblastine kinetically stabilizes microtubules in vitro to such an extent that they can behave essentially as stable nondynamic rods. Such stabilization of microtubule dynamics by vinblastine may be the most sensitive mechanism by which vinblastine blocks cells in mitosis. The vinblastine concentrations used in this study (0.2–1  $\mu\text{M}$ ) were similar to the intracellular concentrations of vinblastine attained when HeLa cells were blocked in mitosis after incubation in culture media containing 2–10 nM vinblastine (Jordan et al., 1991). Importantly, the mitotic spindles of such blocked cells had a full complement of microtubules, and the spindle microtubules and chromosomes either appeared normal by immunofluorescence microscopy or were only subtly disorganized (Jordan et al., 1991, 1992). In many such cells, one or several chromosomes were situated at the spindle poles and appeared to be unable to congress to the metaphase plate. In addition, chromosomes which had successfully congressed to the metaphase plate had significantly fewer microtubules attached to their kinetochores as determined by serial-section electron microscopy (Wendell et al., 1993).

HeLa cell spindles blocked in mitosis by low concentrations of other active Vinca alkaloids and also by low concentrations of nocodazole, podophyllotoxin, colchicine, and taxol also display nearly identical aberrant organizations of chromosomes and microtubules without significant changes in the mass of polymerized microtubules (Jordan et al., 1991, 1992; M. A. Jordan, R. Toso, D. Thrower, and L. Wilson, unpublished results). Such results with low concentrations of vinblastine and the other antimitotic drugs indicate the drugs may inhibit mitosis by stabilizing microtubule dynamics rather than by



excessively depolymerizing or polymerizing spindle microtubules.

During prometaphase, microtubules appear to repeatedly grow and shorten, apparently probing the cytoplasm until they reach and attach to the kinetochores of the chromosomes [e.g., see Rieder et al. (1990) and Hayden et al. (1990)]. Vinblastine-stabilized microtubules could have impaired abilities to reach and become attached to the kinetochores during prometaphase. Such action by vinblastine could explain why some chromosomes in vinblastine-blocked spindles were situated at the poles and why chromosomes that had successfully become aligned at the metaphase plate had fewer than normal numbers of attached microtubules. It is also conceivable that stabilization of the dynamics of the kinetochore and interpolar microtubules is responsible for the inability of the spindles to proceed from metaphase to anaphase. Alternatively, blockage of the transition from metaphase to anaphase may result from inhibition of a cellular signalling event that is dependent on the interaction of dynamic microtubules with the kinetochores (see Jordan et al. (1992)).

#### ACKNOWLEDGMENT

We thank Mr. Herb Miller for preparing the bovine brain microtubule protein.

#### REFERENCES

- Amos, R. D., & Klug, A. (1974) *J. Cell Sci.* 14, 523–549.
- Asnes, C. F., & Wilson, L. (1979) *Anal. Biochem.* 98, 64–73.
- Bayley, P. M., & Martin, S. R. (1991) *Biochem. Soc. Trans.* 19, 1023–1028.
- Bensch, K. G., & Malawista, S. E. (1969) *J. Cell Biol.* 40, 95–107.
- Bradford, M. M. (1976) *Anal. Biochem.* 72, 248–254.
- Carlier, M. F. (1989) *Int. Rev. Cytol.* 115, 139–170.
- David-Pfeuty, T., Simon, C., & Pantaloni, D. (1979) *J. Biol. Chem.* 254, 11696–11702.
- Dustin, P. (1984) *Microtubules*, 2nd ed, Springer-Verlag, Berlin.
- Farrell, K. W., & Wilson, L. (1978) *J. Mol. Biol.* 121, 393–410.
- Farrell, K. W., & Wilson, L. (1984) *Biochemistry* 23, 3741–3748.
- Farrell, K. W., Jordan, M. A., Miller, H. P., & Wilson, L. (1987) *J. Cell Biol.* 104, 1035–1046.
- Gelfand, V., & Bershadsky, A. D. (1991) *Annu. Rev. Cell Biol.* 7, 93–116.
- Gildersleeve, R. F., Cross, A. R., Cullen, K. E., Fagan, A. P., & Williams, R. C., Jr. (1992) *J. Biol. Chem.* 267, 7995–8006.
- Jordan, M. A., & Wilson, L. (1990) *Biochemistry* 29, 2730–2739.
- Jordan, M. A., Margolis, R. L., Himes, R. H., & Wilson, L. (1986) *J. Mol. Biol.* 187, 61–73.
- Jordan, M. A., Thrower, D., & Wilson, L. (1991) *Cancer Res.* 51, 2212–2222.
- Jordan, M. A., Thrower, D., & Wilson, L. (1992) *J. Cell Sci.* 102, 401–416.
- Hayden, J. H., Bowser, S. S., & Reider, C. L. (1990) *J. Cell Biol.* 111, 1039–1046.
- Horio, T., & Hotani, H. (1986) *Nature* 321, 605–607.
- Hotani, H., & Horio, T. (1988) *Cell Motil. Cytoskeleton* 10, 229–236.
- Margolis, R. L., & Wilson, L. (1978) *Cell* 13, 1–8.
- McCormack, J. J. (1990) *Alkaloids* 37, 205–229.
- McIntosh, J. M., & Hering, G. E. (1991) *Annu. Rev. Cell Biol.* 7, 403–426.
- Mitchison, T. J. (1988) *Annu. Rev. Cell Biol.* 4, 527–549.
- Mitchison, T. J. (1989) *J. Cell Biol.* 109, 637–652.
- Mitchison, T., & Kirschner, M. W. (1984a) *Nature* 312, 237–242.
- Mitchison, T., & Kirschner, M. W. (1984b) *Nature* 312, 232–237.
- Na, G. C., & Timasheff, S. N. (1980a) *Biochemistry* 19, 1347–1354.
- Na, G. C., & Timasheff, S. N. (1980b) *Biochemistry* 19, 1355–1365.
- Owells, R. J., Hartke, C. A., Dickerson, R. M., & Haines, F. O. (1976) *Cancer Res.* 36, 1499–1502.
- Rieder, C. L., Alexander, C. L., & Rupp, G. (1990) *J. Cell Biol.* 110, 81–85.
- Rowinsky, E. K., & Donehower, R. C. (1991) *Pharmacol. Ther.* 52, 35–84.
- Scoufias, D. A., & Wilson, L. (1992) *Biochemistry* 31, 738–746.
- Singer, W. D., Jordan, M. A., Wilson, L., & Himes, R. H. (1989) *Mol. Pharmacol.* 36, 366–370.
- Sternlicht, H., & Ringel, I. (1979) *J. Biol. Chem.* 254, 10540–10550.
- Stewart, R. J., Farrell, K. W., & Wilson, L. (1990) *Biochemistry* 29, 6489–6498.
- Timasheff, S. N., Andreu, J., & Na, G. C. (1991) *Pharmacol. Ther.* 52, 191–210.
- Walker, R. A., O'Brien, E. T., Pryer, N. K., Soboeiro, W. A., Erickson, H. P., & Salmon, E. D. (1988) *J. Cell Biol.* 107, 1437–1448.
- Wendell, K. L., Wilson, L., & Jordan, M. A. (1993) *J. Cell Sci.* (in press).
- Wilson, L., & Meza (1973) *J. Cell Biol.* 58, 709–719.
- Wilson, L., & Margolis, R. L. (1981) *Nature* 293, 705–711.
- Wilson, L., & Farrell, K. W. (1986) *Ann. N.Y. Acad. Sci.* 466, 690–708.
- Wilson, L., Anderson, K., & Chin, D. (1976) in *Cold Spring Harbor Conferences on Cell Proliferation: Cell Motility* (Goldman, R., Pollard, T., & Rosenbaum, J. L., Eds) pp 1051–1064, Cold Spring Harbor Laboratory, Cold Spring Harbor, NY.
- Wilson, L., Jordan, M. A., Morse, A., & Margolis, R. L. (1982) *J. Mol. Biol.* 159, 129–149.